Disorder-Induced Coherent Scattering in Slow-Light Photonic Crystal Waveguides

M. Patterson and S. Hughes*
Department of Physics, Queen's University, Kingston, ON K7L 3N6, Canada

S. Combrié, N.-V.-Quynh Tran, and A. De Rossi†
Thales Research and Technology, Route Départementale 128, 91767 Palaiseau CEDEX, France

R. Gabet and Y. Jaouën
Telecom ParisTech, 46 Rue Barrault, 75634 Paris CEDEX 13, France

(Received 12 December 2008; revised manuscript received 27 February 2009; published 25 June 2009)

Light transmission measurements and frequency-delay reflectometry maps for GaAs photonic crystal membranes are presented and analyzed, showing the transition from propagation with a well-defined group velocity to a regime completely dominated by disorder-induced coherent scattering. Employing a self-consistent optical scattering theory, with only statistical functions to describe the structural disorder, we obtain excellent agreement with the experiments using no fitting parameters. Our experiments and theory together provide clear physical insight into naturally occurring light localization and multiple coherent-scattering phenomena in slow-light waveguides.

DOI: 10.1103/PhysRevLett.102.253903 PACS numbers: 42.70.Qs, 41.20.Jb, 42.25.Fx, 42.79.Gn

Introduction.—Photonic crystals (PCs) are periodic dielectric structures that can strongly alter the propagation of light due to the interaction of coherent reflections from the constituent periodic features. In particular, semiconductor-based planar PCs (e.g., Fig. 1) are of great interest due to their ease of fabrication using standard etching and lithography techniques. PC structures can exhibit interesting phenomena such as light trapping on subwavelength spatial dimensions in high-quality cavities [1], or engineered waveguide band dispersions with a vanishing group velocity [2–4]. Both of these effects give rise to novel regimes of light-matter interaction and have broad applications in nano and quantum technologies.

An ongoing challenge is the theoretical description of real fabricated samples, including the generally unknown role of unavoidable structural imperfections, collectively termed "disorder." Indeed, it is now well established that slow-light PC waveguides suffer from significant losses attributed to scattering at disordered surfaces and other device imperfections [5,6]. Rigorous modeling of this generally undesired *extrinsic* scattering phenomena is essential for understanding the underlying physics of measurements and for eventually producing functional devices. However, since the spatial scale of a disordered hole interface is only around 3 nm or less (for ~200 nm holes), and because of the complexity of the structural disorder [7], the theoretical description of light scattering presents enormous challenges.

Previously, Hughes *et al.* [8] introduced a PC waveguide model for *incoherent* extrinsic scattering in the slow-light regime. The incoherent theory predicted the average scattering loss, using a first- and second-order Born approach for the scattering events, with incoherent averaging performed over a large set of nominally identical samples (an ensemble average). The "perturbative" backscattering loss was predicted to scale with the group velocity v_g as $1/v_g^2$ and dominate over scattering into radiation loss modes ($1/v_g$ scaling). Similar scalings were also implied by Povinelli *et al.* [9] and by Gerace and Andreani [10], though the scaling details depend on the nature of the propagating modes and how they sample the disorder regions. These approximate loss-scaling relations have been confirmed experimentally by a number of groups, e.g., [5,11,12], but they may break down at low group velocities where multiple disorder-induced scattering becomes significant [13]. Recent experimental measurements have reported interesting features such as narrow-band resonances near the band edge [6,14] that are not explained at all by the incoherent and perturbative scattering theories (see Fig. 2) and simple v_g scaling rules.

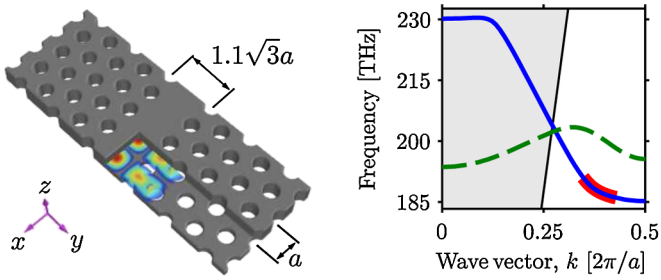

FIG. 1 (color online). Left: Schematic of the planar PC waveguide. A section of the structure is cut away to show the antinodes in the y component of the Bloch-mode electric field. Right: The dispersion relations for the two lowest-order waveguide modes. Only the red highlighted region of the lowest-order (blue, solid) mode is used for the calculations. The grey region at the left represents the continuum of radiation modes above the light line.

In this Letter, we introduce a nonperturbative theory of *coherent* optical scattering. In contrast to previous works, we include unlimited forward- and backscattering events (through a coupled-mode theory), combined with modeling individual, *fully 3D*, disordered waveguides instead of ensemble averages (a statistical average over many disordered waveguides), which is essential for understanding the new experimental observations. The theoretical results are presented alongside measurements on state-of-the-art GaAs PC waveguides which are probed with transmission measurements [15] and optical low-coherence reflectometry (OLCR). OLCR allows the measurement of the back-reflected signal as a function of propagation time inside the PC waveguide. The experimental setup is basically a Michelson interferometer illuminated with a broadband, partially coherent source. The waveguide is placed in one arm and a translating mirror in the other. Properties such as group velocity and complex frequency-dependent reflectance [16] can be extracted from the interference pattern. We also present a powerful and recently developed analytic technique: time-frequency reflectance maps (TFRMs) [6], that can be used to visualize the frequency-dependent impulse response and reveal a number of interesting features such as disorder-induced scattering and facet reflections.

Our formalism also provides fresh insights into the long-standing question of light localization in PC waveguides. It was proposed by John [17] and Anderson [18], that strong localization may be observable in PCs. Although Anderson localization was originally proposed for electrons propagating in a disordered atomic lattice, the phenomena is general to waves in a periodic medium and applicable to PCs. Anderson localization occurs when the mean free path l, of a propagating Bloch mode is reduced to the order of the Bloch wave vector k, totally disrupting propagation; formally $kl < 1$ [19]. There have been a number of milestones towards observing Anderson localization in PCs including the observation of localization in a purely random powder [20], and localization transverse to the propagation direction [21,22]. Recently, Topolancik *et al.* observed resonances at the band edge of an artificially roughened PC waveguide and argued these were due to localization [14]. In contrast, here we report measurements on structures with only *unavoidable disorder*, and provide deeper insight into localization phenomena and the correct criteria for strong localization.

Theory.—In the spirit of a coupled-mode approach, we introduce "slowly-varying envelopes", $\psi_{f[b]}(x)$ for the forward [backward] wave, to approximate the solution as

$$\mathbf{E}(\mathbf{r};\omega) = \mathcal{E}_0[\mathbf{e}_k(\mathbf{r})e^{ikx}\psi_f(x) + \mathbf{e}_k^*(\mathbf{r})e^{-ikx}\psi_b(x)] + \ldots, \tag{1}$$

where "..." includes contributions from lossy radiation modes, $\mathcal{E}_0$ is an amplitude, $\mathbf{e}_k(\mathbf{r})$ is the periodic Bloch-mode electric field normalized by $\int_{\text{cell}} d\mathbf{r}\varepsilon_i(\mathbf{r})|\mathbf{e}_k(\mathbf{r})|^2 = 1$, and k is the wave vector which implicitly depends on the angular frequency ω.

We begin with an ideal structure (no disorder), described through the spatially dependent dielectric constant $\varepsilon_i(\mathbf{r})$, as schematically illustrated in Fig. 1. The structure supports a Bloch waveguide mode (see the solid blue curve in the band structure plot), which exists below the light line (and is thus lossless in the absence of disorder), and which has a group velocity $v_g = d\omega/dk$ that tends to zero at the band edge. If the electric field of the ideal mode $\mathbf{E}_i(\mathbf{r};\omega)$, is incident on a disordered waveguide described by $\varepsilon(\mathbf{r}) = \varepsilon_i(\mathbf{r}) + \Delta\varepsilon(\mathbf{r})$, the exact electric field has a well-known analytical form: $\mathbf{E}(\mathbf{r};\omega) = \mathbf{E}_i(\mathbf{r};\omega) + \int d\mathbf{r}'\overleftrightarrow{\mathbf{G}}(\mathbf{r},\mathbf{r}';\omega)\cdot[\Delta\varepsilon(\mathbf{r}')\mathbf{E}(\mathbf{r}';\omega)]$, where $\overleftrightarrow{\mathbf{G}}(\mathbf{r},\mathbf{r}';\omega)$ is the Green function for the ideal structure. The Green function is obtained from a polarization-dipole solution to Maxwell's electrodynamics equations. By writing $\mathbf{E}(\mathbf{r};\omega)$ as in Eq. (1) and by decomposing the Green function as the superposition of an *exact* bound mode contribution [8] and a radiation modes background summation $\overleftrightarrow{\mathbf{G}}_{\text{rad}}(\mathbf{r},\mathbf{r}';\omega)$, we then derive a pair of coupled-mode equations for the evolution of the envelopes:

$$v_g\frac{d\psi_f(x)}{dx} = ic_{ff}(x)\psi_f(x) + ic_{fb}(x)e^{-i2kx}\psi_b(x) + ic_{fr}(x)\psi_f(x), \tag{2}$$

$$-v_g\frac{d\psi_b(x)}{dx} = ic_{bb}(x)\psi_b(x) + ic_{bf}(x)e^{i2kx}\psi_f(x) + ic_{br}(x)\psi_b(x). \tag{3}$$

The coupling coefficients can be physically interpreted as $c_{ff} = c_{bb}$ driving scattering from a mode into itself, $c_{bf} = c_{fb}^*$ driving scattering into the counterpropagating mode, and c_{fr} and c_{br} driving scattering from the waveguide mode into radiation modes above the light line. We have

$$c_{ff}(x) = \frac{\omega a}{2}\iint dydz\mathbf{e}_k^*(\mathbf{r})\cdot\mathbf{e}_k(\mathbf{r})\Delta\varepsilon(\mathbf{r}), \tag{4}$$

$$c_{bf}(x) = \frac{\omega a}{2}\iint dydz\mathbf{e}_k(\mathbf{r})\cdot\mathbf{e}_k(\mathbf{r})\Delta\varepsilon(\mathbf{r}), \tag{5}$$

$$c_{nr}(x) = \frac{\omega a}{2}\iiint dydzd\mathbf{r}'\Delta\varepsilon(\mathbf{r})\tilde{\mathbf{e}}_{n,k}^*(\mathbf{r})\cdot\overleftrightarrow{\mathbf{G}}_{\text{rad}}(\mathbf{r},\mathbf{r}';\omega)\cdot\tilde{\mathbf{e}}_{n,k}(\mathbf{r}')\Delta\varepsilon(\mathbf{r}'), \qquad n = f, b, \tag{6}$$

where $\tilde{\mathbf{e}}_{f,k}(\mathbf{r}) = \tilde{\mathbf{e}}_{b,k}^*(\mathbf{r}) = \mathbf{e}_k(\mathbf{r})e^{ikx}$, and a is the periodicity of the PC. The most interesting frequency response of the system is dominated by scattering between waveguide modes, through $v_g(\omega)$; while radiative scattering merely leaks energy from the waveguide and is a much smaller effect in the slow-light regime as shown in previous studies. Importantly, this theory accounts for (i) multiple scattering events, (ii) coherent scattering, and (iii) a diminished Bloch-mode amplitude. In addition, we solve the coupled-mode equations numerically for disordered 3D waveguide "instances," in a self-consistent way.

Experimental device.—Except where stated otherwise, the experimental device is a W1.1 PC waveguide fabricated from GaAs as schematically shown in Fig. 1. The width of the waveguide is $1.1\sqrt{3}a$, the pitch is $a = 400$ nm, the thickness is 265 nm, and the hole radius is $R = 0.27a$. The fabrication quality of our GaAs devices is comparable to state-of-the-art silicon processes [23]. The samples were analyzed using the high resolution SEM and the image processing technique of Skorobogatiy *et al.* [7]. The disorder was found to be well described by small perturbations of the radius around the hole perimeter $\Delta R(\phi_\alpha)$, that follow the distribution $\langle \Delta R(\phi_\alpha) \Delta R(\phi'_{\alpha'}) \rangle = \sigma^2 e^{R|\phi_\alpha - \phi'_{\alpha'}|/l_p} \delta_{\alpha,\alpha'}$, where α indexes the holes, and ϕ_α is the angular coordinate of the point. The rms roughness σ, and correlation length l_p, are estimated to be 3 and 40 nm, respectively, and these values are used in our calculations.

Transmission spectra.—An experimental transmission spectrum is shown in the top plot of Fig. 2 for a 1.5 mm W1 waveguide of a different design. Approaching the band edge, the transmission rolls off approximately with $1/v_g^2$, however, there are numerous sharp resonances where the transmission varies by orders of magnitude. Two theoretical models for this waveguide are shown in the bottom plot. The previous incoherent loss calculation [8] (dashed, red), using only a second-order Born approximation, captures the approximate $1/v_g^2$ roll-off but does not explain the resonances. In contrast, the new coherent loss calculation presented in this Letter (solid, blue) reproduces them since it accounts for multiple scattering events which are necessary to build up Fabry-Pérot-like resonance between disorder sites. For reference the group index is shown in the inset (dashed, blue).

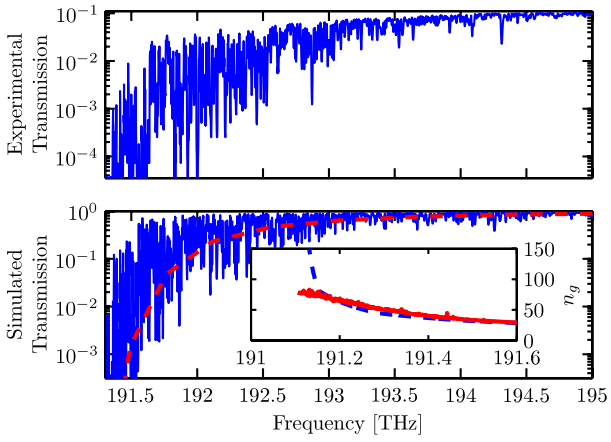

FIG. 2 (color online). Top: Experimental transmission spectra for a 1.5 mm W1 waveguide showing resonances near the band edge. Bottom: Theoretical transmission spectra calculated using the second-order-Born incoherent (dashed, red line) and coherent (solid, blue) scattering theories. Inset: Ideal group index $n_g = c/v_g$ (dashed, blue) compared with an estimate of the effective value due to disorder (red, rough line). The effective group velocity is softened due to disorder and does not diverge like the ideal value. The experimental spectrum is shifted by 1 THz to account for uncertainties with the actual fabricated slab thickness.

While we obtain the general trends of the experiments, over more than 3 orders of magnitude (and without any fit parameters), we have not included the disorder-induced broadening of the slow-light-regime band structure which alters the effective group velocity [24] and softens the roll-off. From a simple perspective, disorder adds or removes dielectric from an unperturbed (to first order) Bloch mode, causing a local frequency shift of the band structure. A propagating mode at fixed frequency thus has a locally varying group velocity due to disorder shifting the waveguide band in frequency. From perturbative calculations with identical disorder statistics, we estimate that the group velocity will be noticeably altered from the ideal value for $v_g \lesssim c/35$ and will have a minimum of around $c/80$ at the band edge, as shown in the inset of Fig. 2 (rough, red). For different structures, this minimum v_g will vary. Although these findings are not important for the reflectance maps analyzed below, our calculations are broadly consistent with our own experiments, those reported by Engelen *et al.* [12], and theoretical analysis of PC coupled-cavity structures [25].

Time-frequency reflectance maps.—TFRMs are intensity plots of the reflected signal as a function of time (horizontal axis) when the structure is excited with a narrow-band pulse centered at some frequency of interest (vertical axis). The map is generated using the complex reflectance of the waveguide which, for physical samples, is deduced from a single set of OLCR data or, for simulated structures, is calculated directly [6].

A simulated TFRM is shown in Fig. 3 for a waveguide with *perfectly transmissive facets*. The dashed blue lines indicate the time the pulse is injected and the round-trip time. The solid magenta line indicates the ideal group index $n_g = c/v_g$ for comparison. Away from the band edge, at higher frequencies, the back reflections are small and are confined between the two time limits, indicating

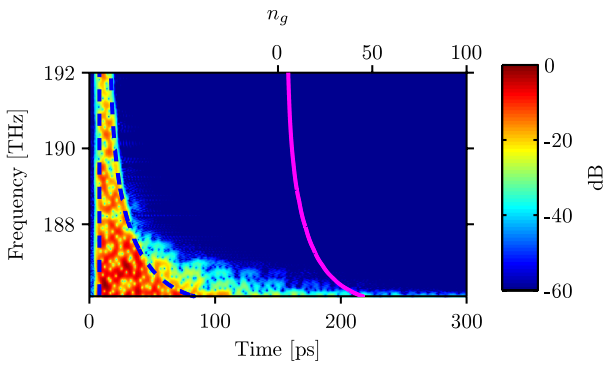

FIG. 3 (color online). A TFRM for a 250 μm simulated disordered waveguide with perfectly transmissive facets showing the strength of the back reflection in dB. The left blue dashed line indicates when the pules was injected and the blue dashed curve is the expected round trip time in an ideal structure. The magenta line shows the group index $n_g = c/v_g$ on the top scale.

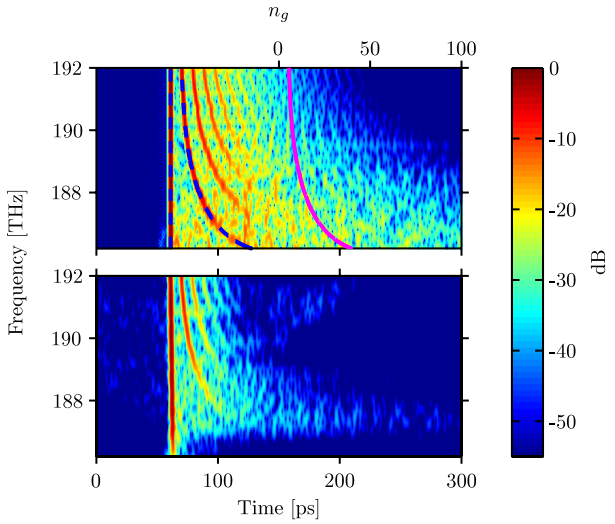

FIG. 4 (color online). Comparison of simulated (top) and experimental (bottom) TFRMs for a 250 μm waveguide with a partially reflective front facet and a strongly reflective back facet. The simulation uses the same disorder configuration as in Fig. 3.

that only single scattering events are occurring. Approaching the band edge, for $v_g < c/20$, scattering becomes significant with strong back reflections and multiple scattering events clearly evidenced by the *hot spots* and the continued reflections after the time for one round trip. This agrees well with Engelen *et al.* [12] who observed total disruption of propagation for $v_g \lesssim c/30$.

Experimental samples have more complicated TFRMs due to reflections from the sample facets. Figure 4 compares simulated (top) and experimental (bottom) TFRMs for the same device geometry. The multiple facet reflections [26] are clearly visible and the time for a round trip lengthens as the group velocity decrease. At low group velocity, the pulse is washed out by strong multiple scattering events, making transmission of signals difficult. Since the simulations do not incorporate details of the experimental setup beyond the sample, they tend to give richer features than the experimental maps. Nevertheless, there is an excellent correspondence between the measured and simulated maps, and this agreement has been found for a number of different sample lengths and facet reflections.

Localization.—Both our measured and simulated transmission spectra (Fig. 1) exhibits sharp resonances near the band edge, similar to those reported in [14]. These features can also be resolved in high resolution TFRMs. To rigorously address the question of whether these features are indicative of localization, a localization length l can be defined as $l^{-1} = -\langle \ln T \rangle / L$ where T is the transmitted power and L is the sample length [27]. For the experimental structure at $k = 0.45 \times 2\pi/a$ where $v_g = c/45$, the localization length is calculated to be $l \sim 100$ μm, giving $kl \sim 700$, which is far from the criterion for strong localization (namely, $kl < 1$). Experimental imaging of light leaking from the waveguide plane confirms that these features are distributed over a large number of waveguide periods. Thus these features are better described as Fabry-Pérot-like resonances between scattering sites and not localization, in agreement with the interpretation of Vlasov *et al.* [27]. This in no way alters the fact that backscattering, and multiple backward and forward scattering, in slow-light modes lead to highly disordered propagation and low transmission.

Conclusion.—By matching several carefully designed light propagation experiments with a new nonperturbative, coherent-scattering formalism, we have demonstrated and explained the crossover from nominal light propagation, with a well-defined group velocity, into a naturally disordered regime that is dominated by coherent scattering and light localization. Our simulated waveguides show excellent qualitative agreement with measurements on GaAs waveguides. We also determine the localization length near the band edge of a PC waveguide and show that while propagation is highly disordered, strong localization is not occurring.

We thank Lora Ramunno, Jeff Young, and John Sipe for useful discussions. This work was supported by the National Sciences and Engineering Research Council of Canada, the Canadian Foundation for Innovation, and the EC project "GOSPEL", Grant No. 219299.

*shughes@physics.queensu.ca
†alfredo.derossi@thalesgroup.com

[1] Y. Akahane *et al.*, Nature (London) **425**, 944 (2003).
[2] M. Notomi *et al.*, Phys. Rev. Lett. **87**, 253902 (2001).
[3] Y. A. Vlasov *et al.*, Nature (London) **438**, 65 (2005).
[4] T. Baba, Nat. Photon. **2**, 465 (2008).
[5] E. Kuramochi *et al.*, Phys. Rev. B **72**, 161318(R) (2005).
[6] A. Parini *et al.*, J. Lightwave Technol. **26**, 3794 (2008).
[7] M. Skorobogatiy *et al.*, Opt. Express **13**, 2487 (2005).
[8] S. Hughes *et al.*, Phys. Rev. Lett. **94**, 033903 (2005).
[9] M. L. Povinelli *et al.*, Appl. Phys. Lett. **84**, 3639 (2004).
[10] D. Gerace *et al.*, Opt. Lett. **29**, 1897 (2004).
[11] L. O'Faolain *et al.*, Opt. Express **15**, 13129 (2007).
[12] R. J. P. Engelen *et al.*, Phys. Rev. Lett. **101**, 103901 (2008).
[13] B. Wang *et al.*, Phys. Rev. B **78**, 245108 (2008).
[14] J. Topolancik *et al.*, Phys. Rev. Lett. **99**, 253901 (2007).
[15] S. Combrié *et al.*, Opt. Express **14**, 7353 (2006).
[16] S. Combrié *et al.*, Appl. Phys. Lett. **90**, 231104 (2007).
[17] S. John, Phys. Rev. Lett. **53**, 2169 (1984).
[18] P. W. Anderson, Philos. Mag. B **52**, 505 (1985).
[19] S. John, Phys. Rev. Lett. **58**, 2486 (1987).
[20] D. S. Wiersma *et al.*, Nature (London) **390**, 671 (1997).
[21] T. Schwartz *et al.*, Nature (London) **446**, 52 (2007).
[22] Y. Lahini *et al.*, Phys. Rev. Lett. **100**, 013906 (2008).
[23] S. Combrié *et al.*, Opt. Lett. **33**, 1908 (2008).
[24] J. G. Pedersen *et al.*, Phys. Rev. B **78**, 153101 (2008).
[25] D. P. Fussell *et al.*, Phys. Rev. B **78**, 144201 (2008).
[26] We use 50% and 100% reflectances for the front and back facets, respectively, to match the sample properties.
[27] Y. A. Vlasov *et al.*, Phys. Rev. B **60**, 1555 (1999).